Real-time functional renormalization group for critical dynamics

Johannes V. Roth and Lorenz von Smekal

Contact: johannes.v.roth@physik.uni-giessen.de

Institut für Theoretische Physik, Justus-Liebig-Universität, 35392 Gießen, Germany

July 2022

Why *real* time?

Performing calculations directly in real time

- avoids the need of an analytic continuation in comparison with the imaginary-time formalism, and
- allows treating phenomena off-equilibrium, e.g. many aspects of heavy-ion collisions, which are very dynamic in nature

Comparison of real-time methods

$$H = \frac{p^2}{2} + \frac{\omega_0^2}{2}x^2 + \frac{\lambda}{4!}x^4$$

Real-time FRG, Gaussian-state approximation, classical-statistical simulations, exact diagonalization of Schrödinger equation, and NLO 2-loop perturbation theory

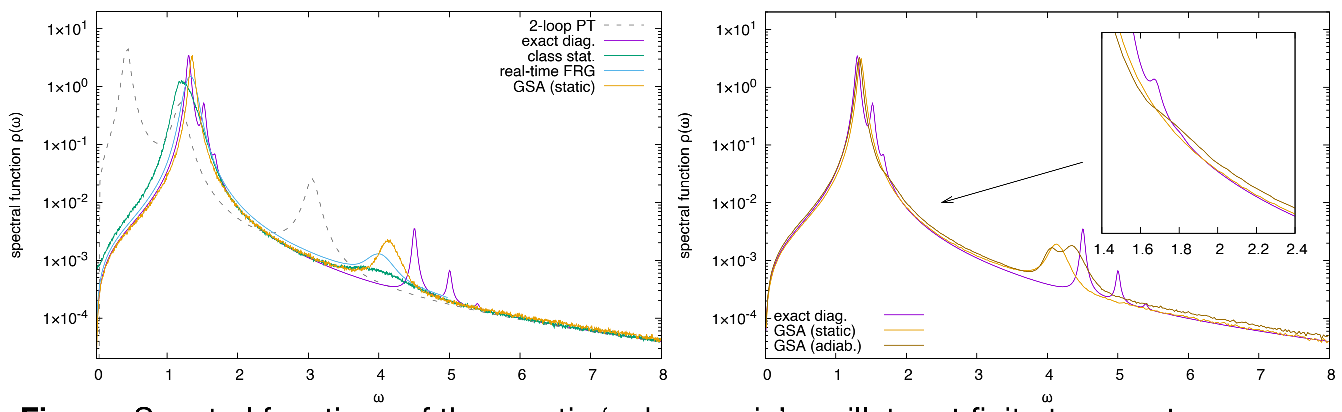

Figure: Spectral functions of the quartic 'anharmonic' oscillator at finite temperature, stemming from various computational techniques, including the real-time FRG [1], here at low temperature $T/\omega_0 = 0.25$, large coupling $\lambda/\omega_0^3 = 4$, and small damping $\gamma/\omega_0 = 0.06$.

Dynamic universality classes

Landau-Ginzburg free energy (statics)

$$F = \int d^d x \left\{ \frac{1}{2}(\vec{\nabla}\varphi)^2 + V(\varphi) + B\varphi n + \frac{n^2}{2\chi_0} + \frac{g}{2}\varphi^2 n \right\}$$

linear Model B coupling

non-linear Model C coupling

Equations of motion (dynamics)

$$\partial_t^2\varphi + \gamma\partial_t\varphi = -\frac{\delta F}{\delta\varphi} + \xi \quad \text{non-conserved}$$

$$\tau_R\partial_t^2 n + \partial_t n = \underbrace{\bar{\lambda}\vec{\nabla}^2\frac{\delta F}{\delta n} + \vec{\nabla}\cdot\vec{\zeta}}_{\text{total divergence (n is conserved density)}}$$

Halperin-Hohenberg classification

$B = 0$, $g = 0$: Model A, $z = 2 + c\eta$
$B > 0$, $g = 0$: Model B, $z = 4 - \eta$ (see Son, Stephanov)
$B = 0$, $g > 0$: Model C, $z = 2 + \alpha/\nu$

Causal regulators

general spectral representation:

$$R_k^{R/A}(\omega, \boldsymbol{p}) = -\int_0^\infty \frac{d\omega'}{2\pi}\frac{2\omega' J_k(\omega', \boldsymbol{p})}{(\omega \pm i\varepsilon)^2 - \omega'^2} - \alpha_k(\boldsymbol{p})k^2$$

(follows directly from Kramers-Kronig relations, when demanding causality)

Constructing regulators in the real-time FRG that comply with the causal analytic (retarded/advanced) structure of the propagators is a non-trivial task [9]. In our work we show that every causal regulator has a spectral representation like above, which can be interpreted as an interaction with a FRG-scale dependent fictitious heat bath [1,2]. Importantly, such a spectral representation entails that causal regulators are *not* UV-finite with respect to frequencies.

Lorentz invariance $J(\omega, \boldsymbol{p}) = \mathrm{sgn}(\omega)\ \theta(p^2)\ \tilde{J}(p^2)$

Example: $\tilde{J}_k(\mu^2) = \dfrac{4k\mu}{(1 + \mu^2/k^2)^2}$

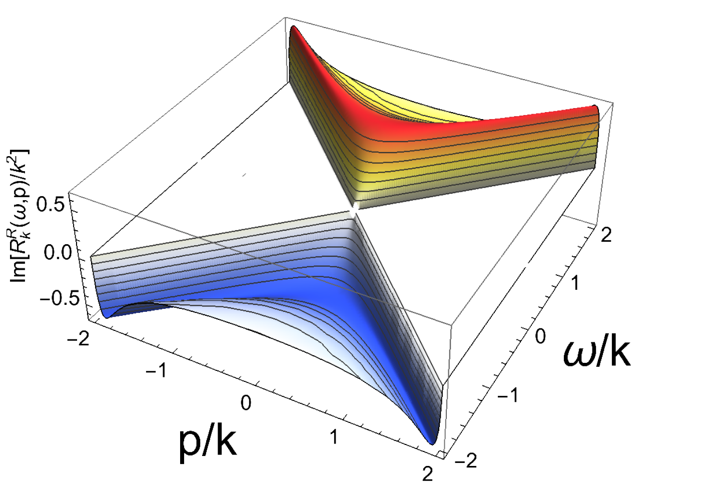

Figure: Imaginary part of the resulting causal, Lorentz invariant, but *not* UV-finite regulator.

flow of retarded propagator poles:

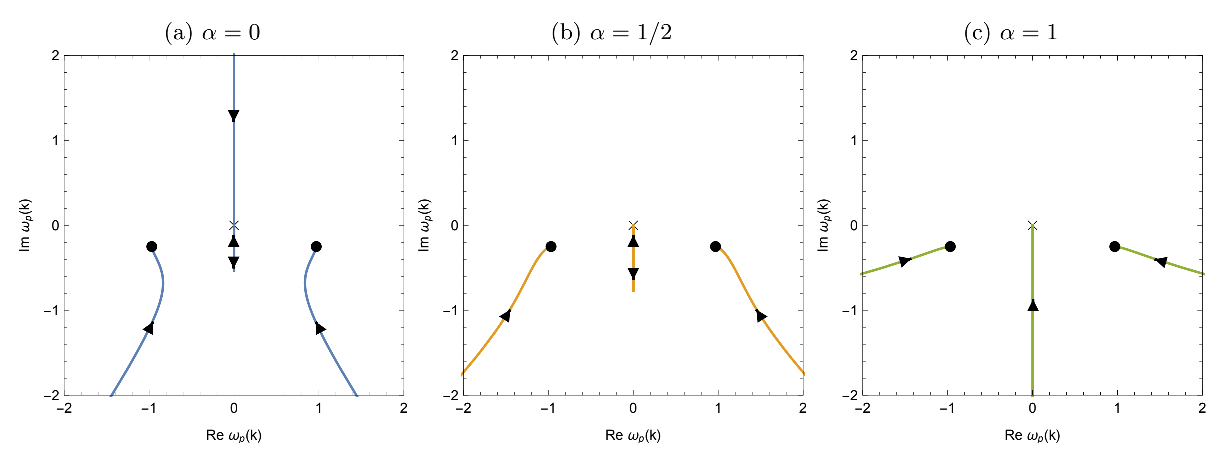

Figure: Trajectories of the poles $\omega_p(k)$ of the retarded propagator in the complex frequency plane for the (0+1)-dimensional quartic 'anharmonic' oscillator, as a function of the FRG scale k. Arrows indicate flow to lower k. The black dots mark the quasiparticle poles when the regulator vanishes. The crosses at the origin mark the point where the regulator-induced third poles disappear for $k \to 0$ in the IR. For $\alpha < 1/2$ (here) this relaxational pole violates causality, as it moves in the upper half plane for sufficiently large values of k.

Truncations for real-time applications

1PI vertex expansion

… around scale-dependent minimum $\phi_{0,k}$ (use for Models A and B)

effective average action:

$$\Gamma_k = \frac{1}{2}\int_{xx'}(\phi^c - \phi^c_{0,k}, \phi^q)_x \begin{pmatrix} 0 & \Gamma_k^{cq}(x,x') \\ \Gamma_k^{qc}(x,x') & \Gamma_k^{qq}(x,x') \end{pmatrix} \begin{pmatrix} \phi^c - \phi^c_{0,k} \\ \phi^q \end{pmatrix}_{x'} - \frac{\kappa_k}{\sqrt{8}}\int_x \left(\phi^c - \phi^c_{0,k}\right)^2 \phi^q - \frac{\lambda_k}{12}\int_x \left(\phi^c - \phi^c_{0,k}\right)^3 \phi^q$$

flow of effective potential:

$\partial_k V_k'(\varphi) = -\dfrac{i}{\sqrt{8}}$ 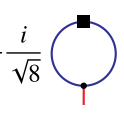

use for squared mass and quartic coupling

flow of 2-point function:

'interaction' with scale-dependent minimum

$\partial_k \Gamma_k^{qc}(x,x') = -i$ 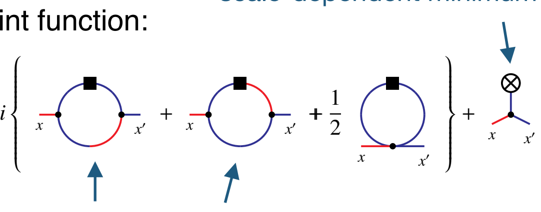

generate non-local power-law behaviour in spectral function

flow of couplings to density: (Model B)

vanish! (coupling is linear ⇝ mixing)

… symmetrically around $\phi = 0$ (use for Models A and C)

effective average action:

$$\Gamma_k = \frac{1}{2}\int_{xx'}(\phi^c, \phi^q)_x \begin{pmatrix} 0 & \Gamma_k^{cq}(x,x') \\ \Gamma_k^{qc}(x,x') & \Gamma_k^{qq}(x,x') \end{pmatrix} \begin{pmatrix} \phi^c \\ \phi^q \end{pmatrix}_{x'} + \frac{3\cdot 2^2}{4!}\int_{xx'} \phi^q(x)\phi^c(x)V_k^{an}(x,x')\phi^q(x')\phi^c(x') + \frac{3\cdot 2}{4!}\int_{xx'} \phi^q(x)\phi^c(x)V_k^{cl,R}(x,x')\phi^c(x')\phi^c(x') + \frac{3\cdot 2}{4!}\int_{xx'} \phi^c(x)\phi^c(x)V_k^{cl,A}(x,x')\phi^q(x')\phi^c(x')$$

flow of 2- and 4-point functions:

$\partial_k \Gamma_k^{qc}(x,x') = -\dfrac{i}{2}$ 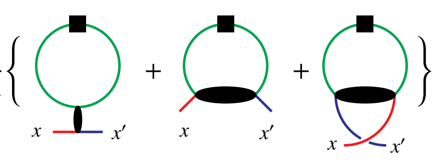

$\partial_k V_k^{cl,R}(x,x') = -i \displaystyle\int_{x-y,\, x'-y'}$ 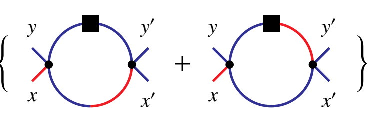

in both cases: expand 2- and 4-point functions in spatial gradients, but keep full frequency dependence:

$$\Gamma_k^{qc}(\omega, \boldsymbol{p}) = \Gamma_{0,k}^{qc}(\omega) - Z_k^\perp \boldsymbol{p}^2 + \cdots$$
$$\Gamma_k^{cq}(\omega, \boldsymbol{p}) = \Gamma_{0,k}^{cq}(\omega) - Z_k^\perp \boldsymbol{p}^2 + \cdots$$
$$\Gamma_k^{qq}(\omega, \boldsymbol{p}) = \frac{2T}{\omega}\left(\Gamma_{0,k}^{qc}(\omega) - \Gamma_{0,k}^{cq}(\omega)\right)$$
$$V_k^{cl,A}(\omega, \boldsymbol{p}) = V_{0,k}^{cl,A}(\omega) + V_{1,k}^{cl,A}(0)\boldsymbol{p}^2 + \cdots$$
$$V_k^{cl,R}(\omega, \boldsymbol{p}) = V_{0,k}^{cl,R}(\omega) + V_{1,k}^{cl,R}(0)\boldsymbol{p}^2 + \cdots$$
$$V_k^{an}(\omega, \boldsymbol{p}) = \frac{2T}{\omega}\left(V_k^{cl,R}(\omega, \boldsymbol{p}) - V_k^{cl,A}(\omega, \boldsymbol{p})\right)$$

flow of couplings to density: (Model C)

$\partial_k g_k = i\sqrt{2}$ 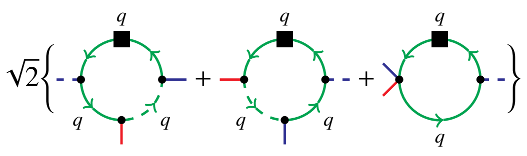

$\partial_k \chi_{0,k}^{-1} = \dfrac{i}{\bar{\lambda}}\lim\limits_{\boldsymbol{p}\to 0}\dfrac{1}{\boldsymbol{p}^2}$ 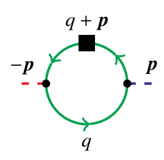

Critical spectral functions of Model A, B, and C

Scaling hypothesis $s^{2-\eta}\rho(s^z\omega, s\boldsymbol{p}, s^{1/\nu}\tau) = \rho(\omega, \boldsymbol{p}, \tau)$

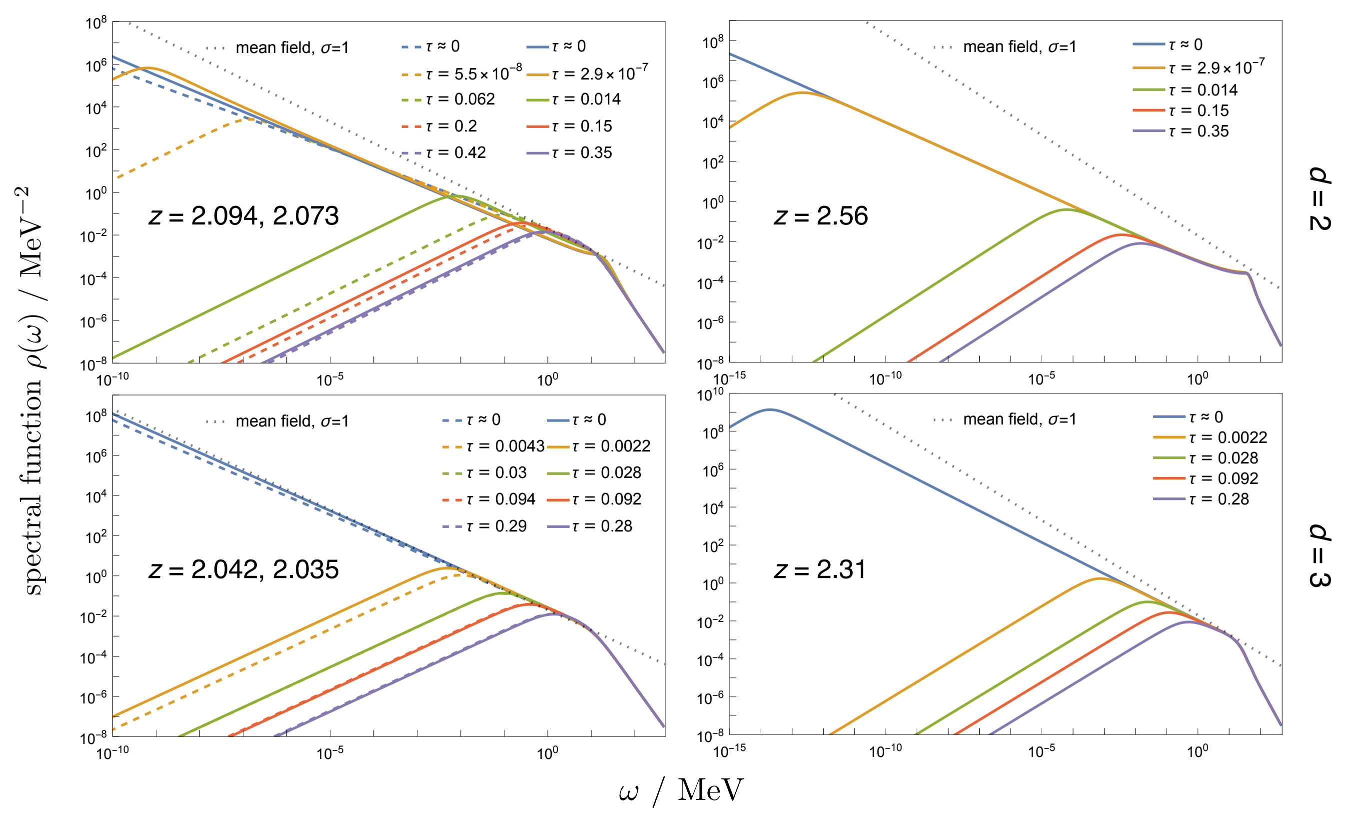

Figure: Critical scaling of the resulting IR ($k \to 0$) spectral functions at vanishing external momentum, gradually building up in the limit $T \to T_c$ of approaching the the critical temperature from above [2]. For analogous results from classical-statistical simulations see also [4].

Figure: Critical spectral function of Model B in three spatial dimensions, realized after Son and Stephanov [8] by coupling a conserved (baryon) density linearly to the non-conserved order parameter. We see that near the critical temperature the order parameter (interpreted as fluctuations of the sigma meson) stays massive. Indeed, it is instead the diffusive mode which emerges as a mixture of fluctuations in the baryon density and fluctuations of the non-conserved sigma meson which becomes critical, giving rise to the critical scaling region at finite spatial momenta. For a treatment of the canonical Model B within classical-statistical simulations see also [5].

Model B (after Son and Stephanov [8])

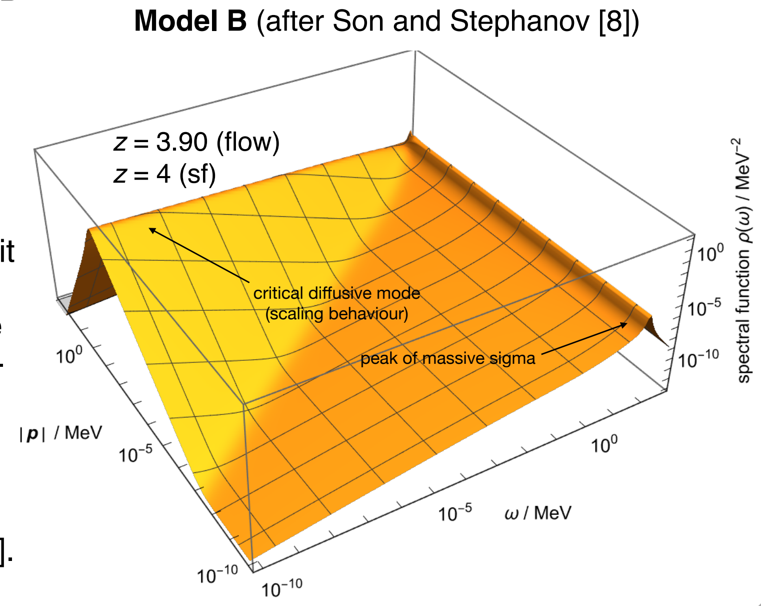

References

[1] J. V. Roth, D. Schweitzer, L. J. Sieke, L. von Smekal, Phys. Rev. D **105**, 116017 (2022)
[2] J. V. Roth, L. von Smekal, in preparation
[3] S. Huelsmann, S. Schlichting, P. Scior, Phys. Rev. D **102**, 096004 (2020)
[4] D. Schweitzer, S. Schlichting, L. von Smekal, Nucl. Phys. B **960**, 115165 (2020)
[5] D. Schweitzer, S. Schlichting, L. von Smekal, arXiv:2110.01696 [hep-lat]
[6] A. O. Caldeira and A. J. Leggett, Physics A **121**, 587 (1983)
[7] P. C. Hohenberg and B. I. Halperin, Rev. Mod. Phys. **49**, 435 (1977)
[8] D. T. Son, M. A. Stephanov, Phys. Rev. D **70**, 056001 (2004)
[9] C. Duclut and B. Delamotte, Phys. Rev. E **95**, 012107 (2017)

DFG CRC-TR 211 Strong-interaction matter under extreme conditions
HGS-HIRe for FAIR Helmholtz Graduate School for Hadron and Ion Research
HFHF Helmholtz Forschungsakademie Hessen für FAIR
JUSTUS-LIEBIG-UNIVERSITÄT GIESSEN